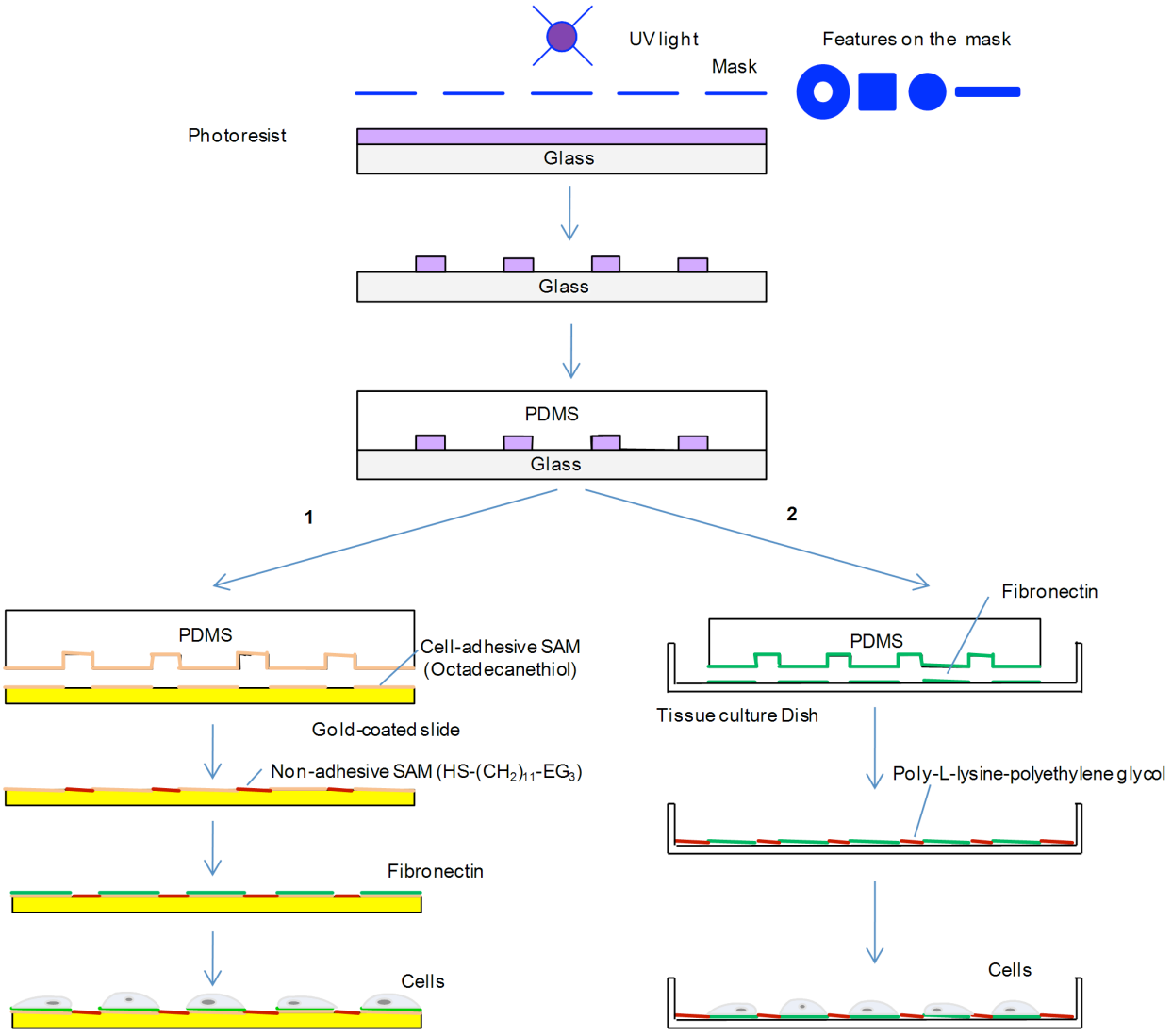

Figure S1. Micro-fabrication and micro-contact printing for cell patterning. A negative photoresist mold was made first by UV (ultraviolet) crosslinking through a mask containing desired micropatterning features. PDMS (polydimethylsiloxane) elastomeric stamps were then casted with prepolymers onto the mold. In most experiments (**path 1**), octadecanethiol, an adhesive self-assembly monolayer (SAM), was transferred via the PDMS stamp onto gold-coated glass slides, which were then sequentially subjected to a non-adhesive ethylene glycol-terminated SAM HS-$(CH_2)_{11}$-EG_3 and fibronectin. Alternatively (**path 2**), fibronectin was stamped onto tissue culture treated plastic, which was subsequently backfilled with poly-L-lysine-polyethylene glycol and washed with PBS for cell seeding.

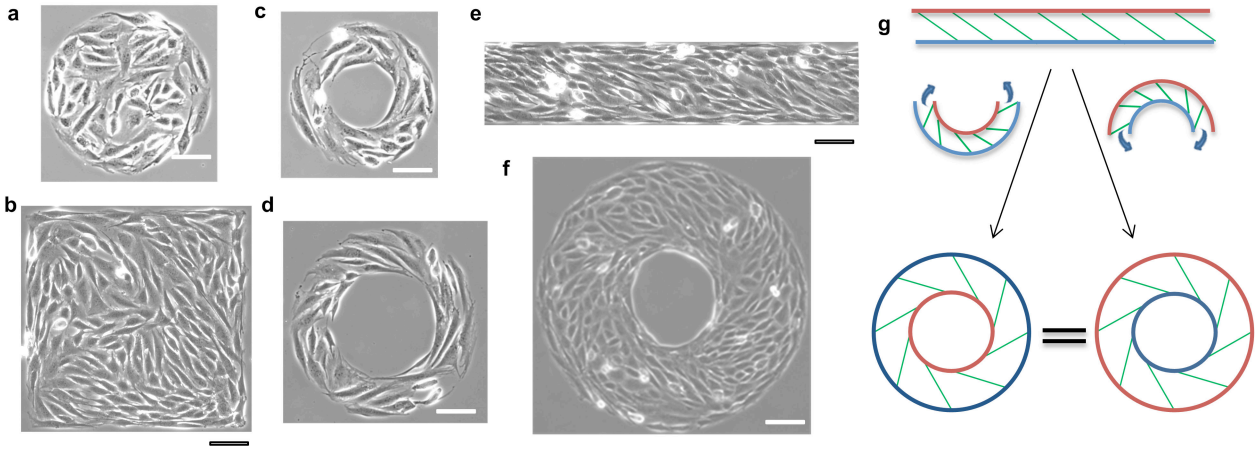

Figure S2. C2C12 cells grown on micro-patterned surfaces. (**a-f**) Cells on strip and ring geometries clearly demonstrate asymmetric alignment, while those residing on the circular and square patterns do not. (**g**) A schematic of the conformity in the biased cell alignment between cells on strips and cells on rings. Green lines indicate the direction of cell alignment, while blue and red lines represent the opposite boundaries of strips or rings. Ring geometry shows a consistent biased alignment regardless of whether the linear strip was bent upward or downward to create ring geometry, suggesting that the left-right asymmetry is independent of the ring curvature. Scale bars: 100 μm.

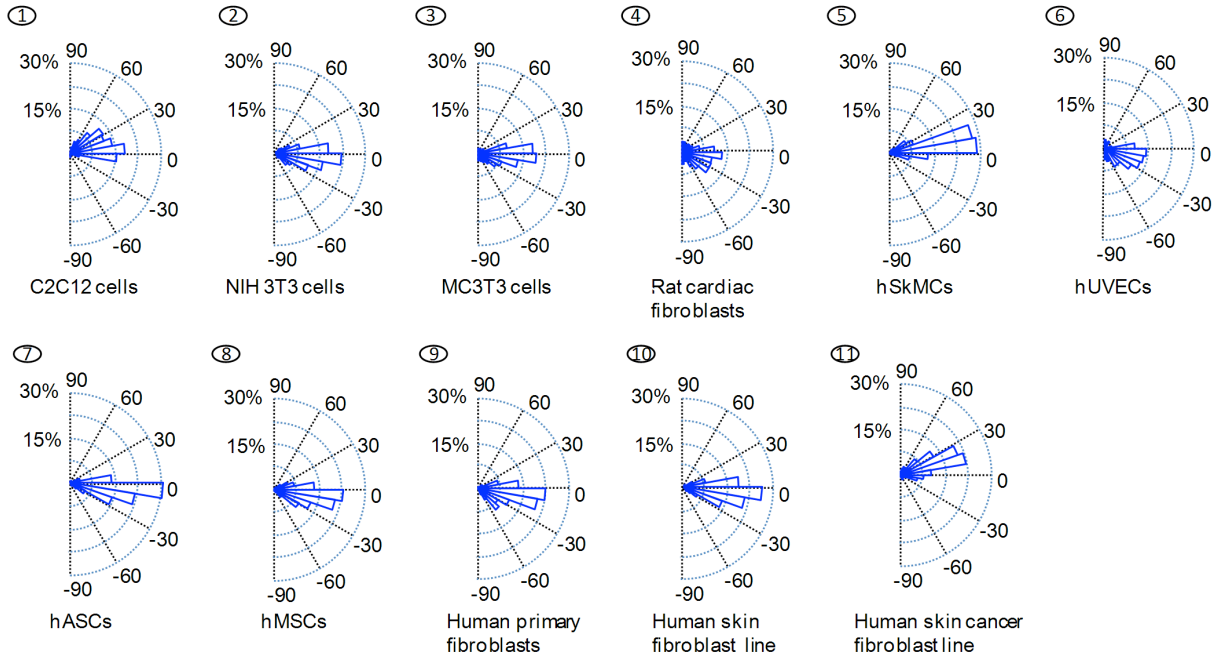

Figure S3. Circular histograms of biased angles in the phase contrast images of different cell types (shown in Figure 2a)**.**

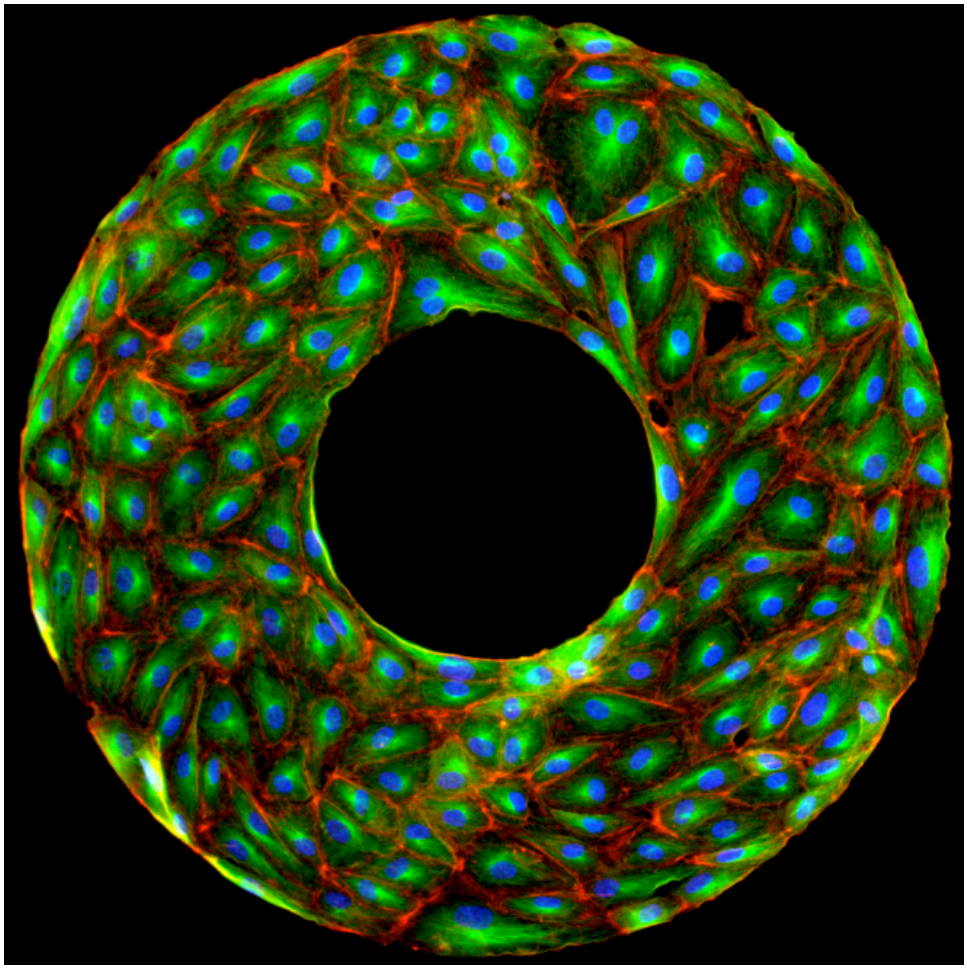

Figure S4. Centrosome positioning of hUVECs on a micropatterned ring (inner ring: 250 μm and width: 200 μm). Centrosomes (bright green) are positioned closer to each boundary than nuclei (blue) in hUVECs (actin: red, tubulin: green).

a

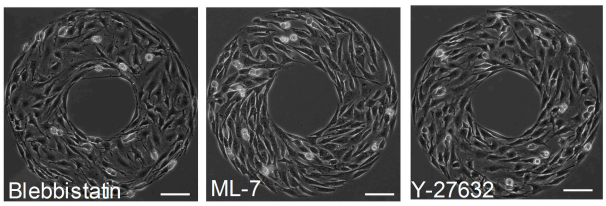

b

C2C12 Drug	Num of Exps	CW	N/S	CCW	p Value
Control	2	0	0	73	$1.1X10^{-22}$
Blebb	2	0	11	17	$7.6X10^{-6}$
ML-7	2	0	4	19	$1.9X10^{-6}$
Y-27632	3	0	7	22	$2.4X10^{-7}$

Figure S5. Effects of drugs blocking the actomyosin motor. Phase contrast images (**a**) and chirality data (**b**) of C2C12 cells under the treatment of drugs that affect the function of actomyosin motor. These drugs (Blebbistatin, ML-7, and Y-27632) did not affect left-right asymmetry. Scale bars: 100 μm.

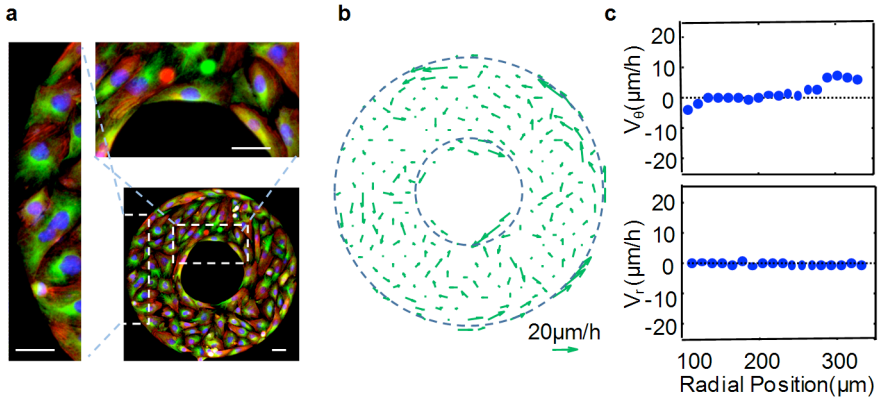

Figure S6. C2C12 cell polarization, alignment, and migration on micropatterned rings with 200nM Nocodazole. (**a**) Nocodazole does not change the polarity of C2C12 cells, as the cells positioned their centrosome (bright green), rather than the nucleus (blue), closer to ring boundaries. Scale bars: 50 μm. (**b**) Migration of C2C12 cells in the presence of Nocodazole, with the direction and magnitude of velocity indicated by arrow direction and length, respectively. (**c**) Average velocity of the cells along the circumferential direction (V_θ) and the radial direction (V_r) as a function of radial position.

Table S1 Compositions of cell culture media

Cell Type	Base Medium Source	Composition
C2C12	Invitrogen Cat# 21068	DMEM with 10% FBS, 1% P/S, 1mM sodium pyruvate
hUVEC	Lonza Cat# CC-3156 Cat# CC-4176	Endothelial Basal Medium-2 (EBM-2) supplemented with EGM-2 SingleQuot Kit supplement & growth factors
NIH/3T3	Invitrogen Cat# 21068	DMEM with 10% FBS, 1% P/S, 1mM sodium pyruvate
hASC	Invitrogen Cat# 21068	DMEM with 10% FBS, 1% P/S, 1mM sodium pyruvate
hMSC	Invitrogen Cat# 21068	DMEM with 10% FBS, 1% P/S, 1mM sodium pyruvate
hSkMC	Lonza Cat# CC-3161 Cat# CC-3160	SkMC Basal Media supplemented with SkMC SingleQuot Kit supplement & growth factors
MC-3T3	Invitrogen Cat# 12561	Minimum essential α Medium with 10% FBS, 1% P/S
Human primary skin fibroblast	Invitrogen Cat# 21068	DMEM with 10% FBS, 1% P/S, 1mM sodium pyruvate
Human skin fibroblast line	Invitrogen Cat# 21068	DMEM with 10% FBS, 1% P/S, 1mM sodium pyruvate
Rat cardiac fibroblast	Invitrogen Cat# 21068	DMEM with 10% FBS, 1% P/S, 1mM sodium pyruvate

DMEM: Dulbecco's Modified Eagle Medium; P/S: penicillin/streptomycin; and FBS: fetal bovine serum; C2C12: mouse skeletal muscle C2C12 cell line; hUVEC: human umbilical vein endothelial cells; NIH/3T3: mouse embryonic fibroblast cell line; hASC: human adipose-derived stem cells; hMSC: human bone marrow-derived mesenchymal stem cells; hSkMC: human skeletal muscle cell line; MC-3T3: mouse osteoblast cell line.

Tables S2 - S3. The chirality of mouse myoblast cell line C2C12 (Table S2, left) and human umbilical vein endothelial cells, hUVECs (Table S3, right) on ring patterns.

C2C12	CW	N/S	CCW	Biased?	p Value
1	0	1	21	Y	$4.8X10^{-7}$
2	0	2	37	Y	$7.3X10^{-12}$
3	2	7	29	Y	$2.3X10^{-7}$
4	0	4	18	Y	$3.8X10^{-6}$
5	0	1	25	Y	$3.0X10^{-8}$
6	0	1	28	Y	$3.7X10^{-9}$
7	0	3	19	Y	$1.9X10^{-6}$
8	0	2	25	Y	$3.0X10^{-8}$
9	0	0	28	Y	$3.7X10^{-9}$
10	0	0	45	Y	$2.8X10^{-14}$
11	0	2	27	Y	$7.5X10^{-9}$
12	0	4	31	Y	$4.7X10^{-10}$
13	6	29	29	Y	$5.8X10^{-5}$
14	4	27	8	N	0.19
15	3	7	21	Y	$1.4X10^{-4}$
16	0	2	10	Y	$9.8X10^{-4}$
17	0	0	21	Y	$4.8X10^{-7}$
18	0	6	29	Y	$1.9X10^{-9}$
19	3	4	19	Y	$4.3X10^{-4}$
20	0	7	7	Y	$7.8X10^{-3}$
21	2	7	37	Y	$1.4X10^{-9}$
22	4	8	11	Y	0.04
23	1	4	27	Y	$1.0X10^{-7}$
24	1	6	35	Y	$5.2X10^{-10}$
25	0	3	28	Y	$3.7X10^{-9}$
26	1	3	28	Y	$5.4X10^{-8}$
27	0	4	36	Y	$1.5X10^{-11}$
28	1	5	42	Y	$4.9X10^{-12}$
29	2	7	21	Y	$3.0X10^{-5}$
30	1	6	27	Y	$1.0X10^{-7}$
31	3	8	36	Y	$1.7X10^{-8}$
32	0	1	21	Y	$4.7X10^{-7}$
33	0	1	24	Y	$6.0X10^{-8}$
Sum	34	172	850	Y	$1.6X10^{-254}$

hUVEC	CW	N/S	CCW	Biased?	p Value
1	17	0	0	Y	$7.6X10^{-6}$
3	13	7	4	Y	0.018
4	22	2	1	Y	$2.7X10^{-6}$
5	31	6	1	Y	$7.5X10^{-9}$
6	10	1	0	Y	$9.8X10^{-4}$
7	25	14	2	Y	$2.6X10^{-6}$
8	15	4	1	Y	$2.4X10^{-4}$
9	35	8	2	Y	$4.8X10^{-9}$
10	26	6	1	Y	$2.0X10^{-7}$
11	26	4	0	Y	$1.5X10^{-8}$
12	24	4	1	Y	$7.5X10^{-7}$
13	34	7	1	Y	$1.0X10^{-9}$
14	29	2	2	Y	$2.2X10^{-7}$
Sum	307	65	16	Y	$2.7X10^{-71}$

CW: clockwise alignment, CCW: counter-clockwise alignment, and N/S: not significantly biased to CW or CCW.